Supporting Information

Regulating the local microenvironment on porous Cu nanosheets for enhancing electrocatalytic CO_2 reduction selectivity to ethylene

Dan Wang,[a b 1] Qingqing Song,[a 1] Kaibin Li,[b] Yuwei Zhou,[a] Junjun Mao,[a] Chenchen Zhang,[a] Yang Lou,[a] Chengsi Pan,[a] Jiawei Zhang,[a] Yongfa Zhu,[c] and Ying Zhang*[a]

[a] *Key Laboratory of Synthetic and Biological Colloids Ministry of Education, School of Chemical and Material Engineering, Jiangnan University, Wuxi, Jiangsu 214122, China*

[b] *Shaanxi Engineering Research Center for Mineral Resources Clean & Efficient Conversion and New Materials, Shaanxi Key Laboratory of Comprehensive Utilization of Tailings Resources, College of Chemical Engineering and Modern Materials, Shangluo University, Shangluo 726000, China*

[c] *Department of Chemistry, Tsinghua University, Beijing 100084, China*

1. Experimental Procedures

1.1 Instrumentation. X-ray diffraction (XRD) patterns were recorded on a Bruker AXS D8 diffractometer using Cu Kα radiation (λ=0.15406 nm) with a scanning rate of 4° min^{-1}. The morphology and microscopic features of the samples were investigated on a Hitachi S-4800 scanning electron microscope (SEM) and JEM-2100 plus transmission electron microscopy (TEM). The liquid product was analyzed by ^1H NMR experiments using a Bruker AVANCE III HD 400 MHz spectrometer at frequencies of 400.2 MHz. The gaseous products were analyzed by Gas Chromatograph (GC 2060, Shanghai Ruimin Instrument Co., LTD). The X-ray photoemission spectroscopy (XPS) analysis was carried out with an AXIS Supra (Kratos, UK) using monochromatized Al Kα radiation (hv = 1486.6 eV, 225 W) as the X-ray source and all spectra were calibrated with C 1s (284.8 eV). The related electrochemical tests in this work were done on an electrochemical workstation (CHI 660E) at room temperature and pressure unless specifically noted otherwise. The contact angle of CO gas on the electrode surface was measured using the bubble capture method. The surface of the electrode was illuminated using a fiber-optic illumination system (CEL-TCX 250), and the attachment of CO gas bubbles to the electrode surface was recorded using a microscope (SZX16, Olympus) installed on a high-speed CCD camera (i-SPEED 3, AOS Technologies) to analyze the wettability of CO on the electrode surface.

* To whom correspondence should be addressed.
Email: ying.zhang@jiangnan.edu.cn

1.2 Electrocatalytic CO_2 reduction measurements. The electrolysis process was performed in a flow cell configuration. The flow cell configuration (shown in **Fig. S1a**) was made up of a gas-diffusion layer (H29BC, Sigracet) coating the catalyst, and a Pt mesh (1.2 cm × 1.5 cm, 0.5 mm thickness) used as the anode electrode and a cathode electrode. An anion exchange membrane separated the cathode and anode cells (X37-50 Grade T, Dioxide Materials). These three components were positioned and clamped together using polytetrafluoroethylene (PTFE) spacers. The Ag/AgCl (3.5 M KCl) was used as the reference electrode. All potential measurements were converted to the RHE based on the formula: E (V *vs.* RHE) = E (V *vs.* Ag/AgCl) + 0.0591 V × pH + 0.205 V. The potentials (V vs RHE) were estimated using the pH value of the electrolyte exiting the flow cell configuration. The pH value of the 1 M KOH is about 14. The CO_2 flow was controlled at 25 sccm by an ALICAT mass flow controller. The electrolyte was circulated through the electrochemical cell by a peristaltic pump (BQ 80S, Lead Fluid) with a flow rate of 11 mL min^{-1}. All the electrolysis measurements were powered by an electrochemical workstation (CS310H, Wuhan Corrtest Instruments Corp., Ltp) at room temperature and pressure. The gaseous products were analyzed using a gas chromatograph. 1H Nuclear Magnetic Resonance Spectroscopy quantitatively analyzed the liquid product with 500 μL electrolyte mixed with 200 μL D_2O and 100 μL DMSO with a specific concentration used as an internal standard.

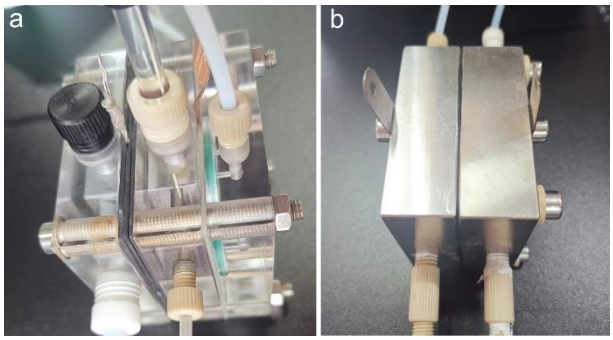

Figure S1 The optical photograph of (a) flow cell configuration and (b) MEA electrolyzer used in this work.

The membrane electrode assembly (MEA) electrolyzer consisted of a cathode electrode (with a working area of 2.25 cm^2), an anion-exchange membrane (Sustainion X37-50 RT), and an anode electrode (IrO_2-Ti mesh) used for the preliminary evaluation of the stability of the porous Cu NSs in ECO_2RR process, as shown in **Fig. S1b**. 20 mg porous CuO NSs, 5 mg Ketjenblack, and 5 μL 5 wt% Sustainion XA-9 ionomer solution were dispersed into 2 mL ethanol under sonication for about 5 h to form a homogeneous cathode catalyst ink. The cathode was prepared by spraying the prepared catalyst ink on a 1.5 *1.5 cm^2 GDL (H29BC, Sigracet) with a catalyst loading of about 1.5 mg cm^{-2}. The anode electrode was prepared based on the previous report[1]. The CO_2 flow was controlled

at 50 sccm by a mass flow controller. The electrolyte (0.1 M $KHCO_3$ aqueous solution) was circulated through the electrochemical cell by peristaltic pumps (BQ 80S, Lead Fluid) with a flow rate of 20 mL min^{-1}. Stability tests were performed at a constant full cell potential of −3.3V, powered by an electrochemical workstation (CS310H, Wuhan Corrtest Instruments Corp., Ltp) at room temperature and pressure.

2. Supplemental Figures and discussion

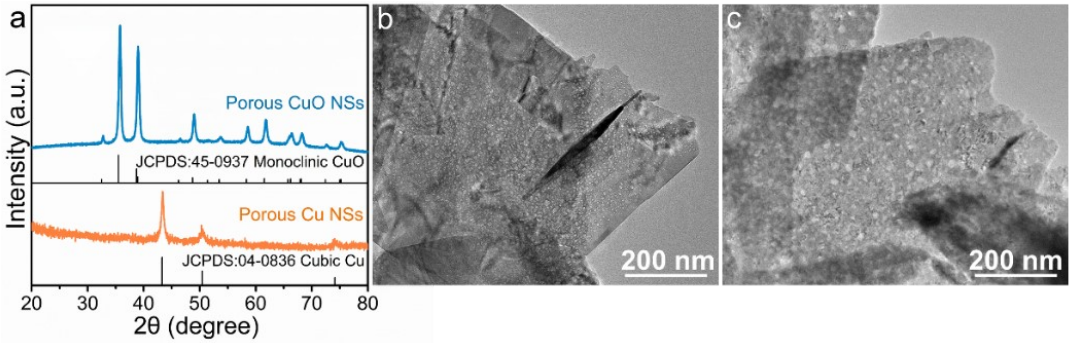

Figure S2 (a) XRD patterns of porous CuO NSs and their electroreduced porous Cu NSs. TEM images of (b) porous CuO NSs and (c) their electroreduced porous Cu NSs.

The electroreduction process provides a mild reduction condition, in which a controllable amount of electrons are constantly provided at a suitable cathodic applied potential. The slow conversion kinetics can keep the porous nanosheet morphology. In this work, the copper oxide nanosheets are reduced to copper via in situ electroreduction while applying negative potential for CO_2 reduction. During the electroreduction process, O atoms were dynamically removed from CuO while the Cu skeleton remained. **Fig. S2a** shows the XRD patterns of porous CuO NSs and the porous Cu NSs obtained after the ECO_2RR process, indicating that the monoclinic phase CuO can be completely transformed into the cubic phase Cu with high purity. The TEM images of porous CuO NSs and their electroreduced porous Cu NSs are shown in **Fig. S2b**, **c**, both of which maintain a porous nanosheet-like structure, indicating that the structural skeleton of the precursor porous CuO NSs can be stable during the in situ electrochemical reduction process.

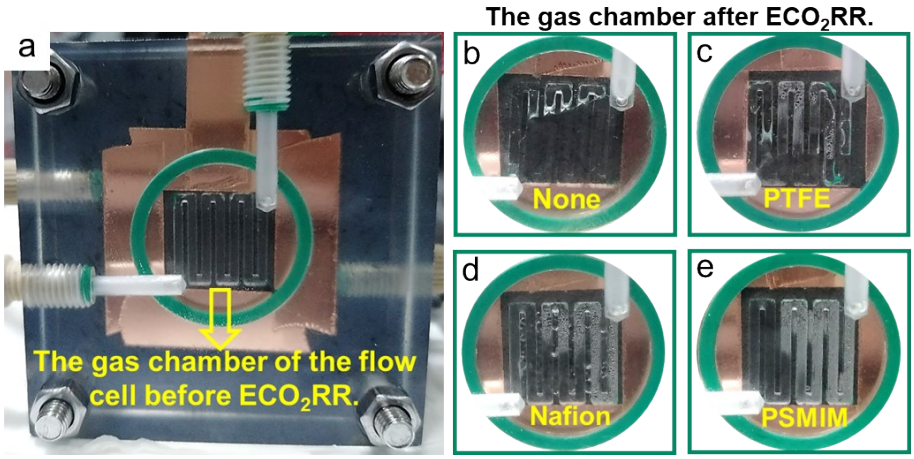

Figure S3 (a) A photograph of the gas chamber side of the flow electrolyzer. (b) Photograph of the gas chamber side after ECO_2RR of the porous Cu NSs electrode without modification. Photographs of the gas chamber side after ECO_2RR on (c) PTFE-Cu NSs, (d) Nafion-Cu NSs, and (e) PSMIM-Cu NSs.

Fig. S3a shows a photograph of the gas chamber side of the flow cell before ECO_2RR. **Figs. S3b-e** shows photographs of the gas chamber side of porous Cu NSs electrodes without organic polymer modification (None-Cu NSs), and with PTFE-, Nafion-, and PSMIM-modified porous Cu NSs (PTFE-Cu NSs, Nafion-Cu NSs, and PSMIM-Cu NSs), respectively, after a period of ECO_2RR. The None-Cu NSs electrode was almost completely submerged in the electrolyte after about 1.5 hours of electrolysis (**Fig. S3b**), resulting in a sharp decrease in ECO_2RR efficiency. Introducing non-ionic hydrophobic organic polymer PTFE can improve the problem of GDE being submerged in water. After 2 hours of electrolysis, only a partial area of the gas chamber side of the PTFE-Cu NSs electrode was submerged (**Fig. S3c**). When the porous Cu NSs electrode was modified with cationic organic polymer Nafion (**Fig. S3d**), the problem of GDE being submerged in water was significantly improved, with only a small amount of liquid present on the gas chamber side after about 1.5 hours of electrolysis. When the porous Cu NSs electrode was further modified with anionic organic polymer PSMIM (**Fig. S3e**), the problem of GDE being submerged was further improved, with only partial water vapor present on the gas chamber side after 4 hours of electrolysis, without obvious water submersion.

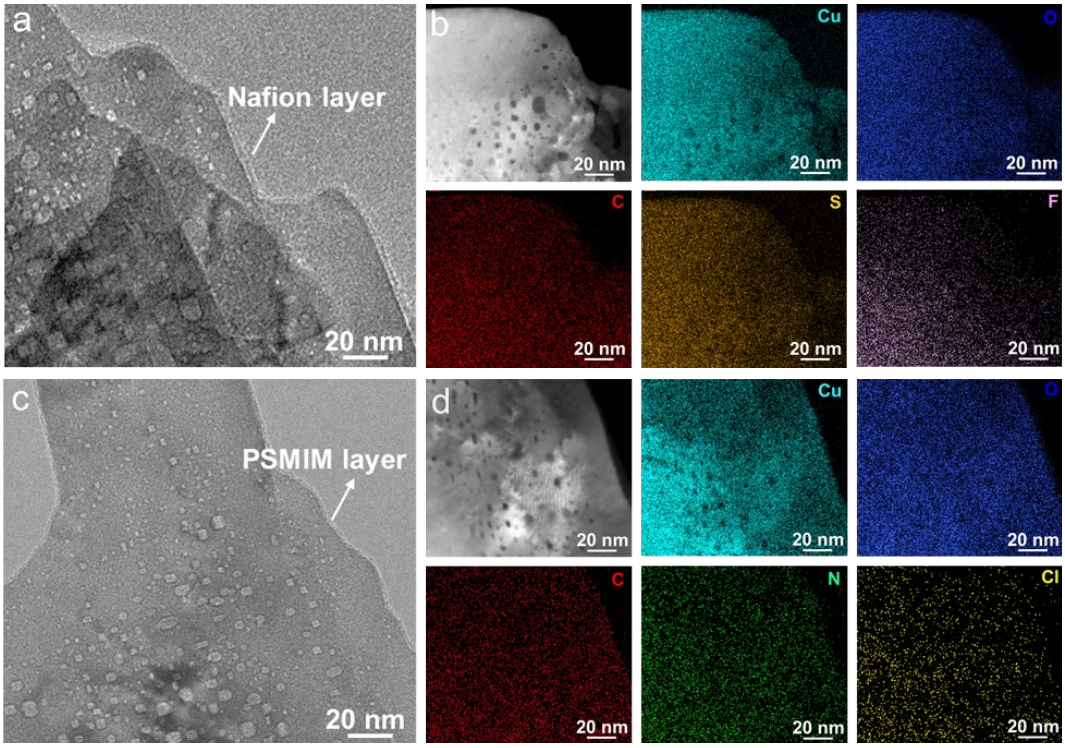

Figure S4 The TEM images of porous CuO NSs modified with (a) Nafion and (c) PSMIM. The STEM images of porous CuO NSs modified with (b) Nafion and (d) PSMIM, the element distributions on their surfaces, respectively. Cu (cyan), O (blue), C (red), S (orange), F (pink), N (green), and Cl (yellow).

Figs. S4a and **c** show TEM images of Nafion- and PSMIM-modified porous CuO NSs, respectively, clearly showing that the surface of the porous CuO NSs is uniformly coated with an organic polymer layer. Further verification was conducted using scanning transmission electron microscopy - X-ray energy dispersive spectroscopy, which confirmed that Nafion and PSMIM can be uniformly attached to the surface of porous CuO NSs. As shown in **Fig. S4b**, when Nafion is added, Cu, O, C, S, and F elements are evenly distributed on the surface of porous CuO NSs. **Fig. S4d** shows that when PSMIM is added, Cu, O, C, N, and Cl elements are evenly distributed on the surface of CuO NSs.

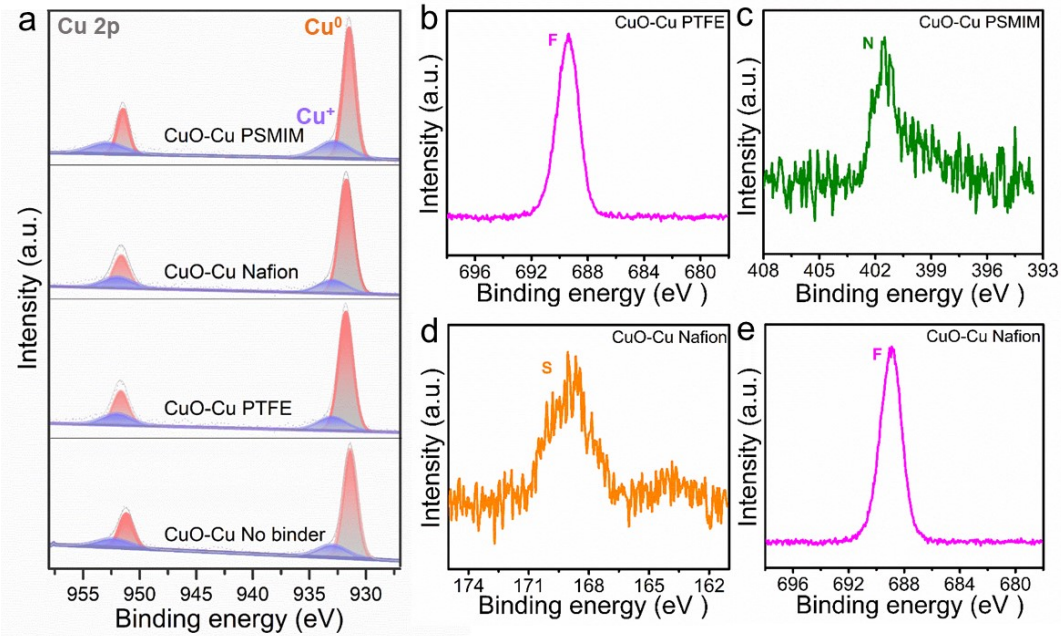

Figure S5 XPS spectra of (a) Cu 2p, (b) F 1s (PTFE), (c) N 1s (PSMIM), (d) S 2p, and (e) F 1s (Nafion).

After in-situ electroreduction, porous CuO NSs modified with different types of organic polymers can be converted into porous Cu NSs, which can be used for electrocatalytic CO_2 reduction. To demonstrate that the organic polymers attached to the surface of porous Cu NSs obtained by in-situ electroreduction can remain stable during the ECO_2RR process, X-ray photoelectron spectroscopy (XPS) analysis was conducted on different types of organic polymer-modified porous Cu NSs electrodes after one hour of ECO_2RR. **Figure S5a** shows the Cu 2p XPS spectrum of porous Cu NSs electrodes modified with different organic polymers. The high-intensity peaks at ~932.7 and ~952.1 eV are associated with Cu^0, while the low-intensity peaks at ~933.3 and ~952.9 eV are associated with Cu^+. As porous Cu NSs are susceptible to oxidation by air, a small amount of Cu_2O was detected on the surface of the electrode by non-in situ XPS testing. Furthermore, the absence of characteristic diffraction peaks of Cu_2O in the XRD pattern of porous Cu NSs (**Figure S2a**) further demonstrates that only the surface of porous Cu NSs is oxidized by air and contains a small amount of Cu_2O. In addition, no Cu-C or Cu-N bonds were detected, indicating that the added organic polymers do not form covalent bonds with porous Cu NSs. Characteristics of elements F, N, Cl, and S were detected in the XPS spectra of porous Cu NSs electrodes modified with PTFE, PSMIM, and Nafion, respectively, (**Figures S5b-e**), indicating that the structure of the organic polymers attached to the surface of porous Cu NSs can remain stable during the ECO_2RR process.

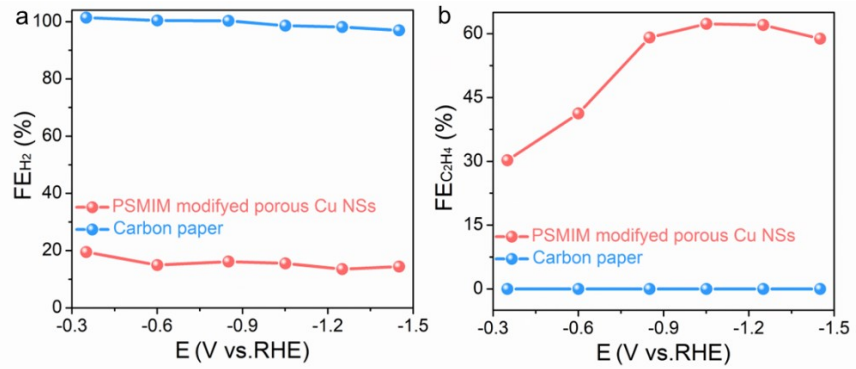

Figure S6 The FEs for H_2 (a), and (b) the FEs for C_2H_4 on hydrophobic carbon paper PSMIM modified porous Cu NSs electrode.

Only hydrogen evolution reaction occurs on the hydrophobic carbon paper, indicating that the carbon paper used in this work did not affect the selectivity of carbon-based products in the ECO_2RR process.

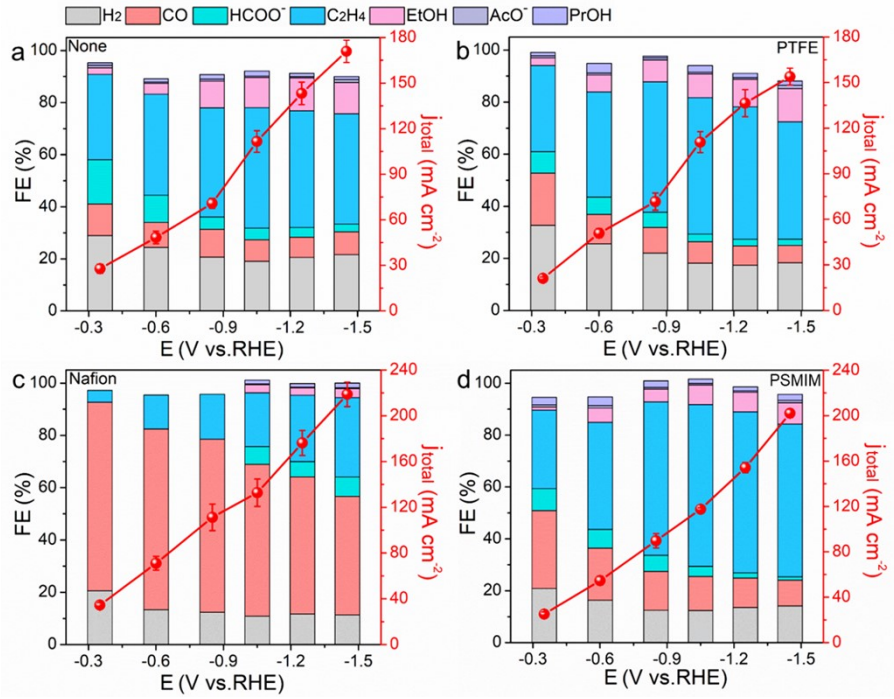

Figure S7 FEs for ECO_2RR products on porous Cu NSs modified by different organic polymers.

Fig.S8a compares the FEs of H_2 produced from CO_2 electroreduction on different types of organic polymer-modified porous Cu NSs electrodes under different applied potentials. The None-Cu NSs electrode exhibits the highest selectivity for H_2 production, as the electrolyte can easily penetrate the catalyst layer of the None-Cu NSs electrode, resulting in competing hydrogen evolution reactions (HER). The PTFE-Cu NSs electrode has lower selectivity for H_2 production. In contrast, the PSMIM-Cu NSs and Nafion-Cu NSs electrodes further suppress the HER side reaction, leading to further reduction of the H_2 FE. **Fig. S8b** compares the partial current densities of the main

products obtained from CO_2 electroreduction on different types of organic polymer-modified porous Cu NSs electrodes under different applied potentials. The Nafion-Cu NSs electrode exhibits high efficiency for CO production, while the PSMIM-Cu NSs electrode has high efficiency for C_2H_4 production. These results indicate that organic polymer modification plays a vital role in enhancing the efficiency and selectivity of CO_2 electroreduction on porous Cu NSs electrodes.

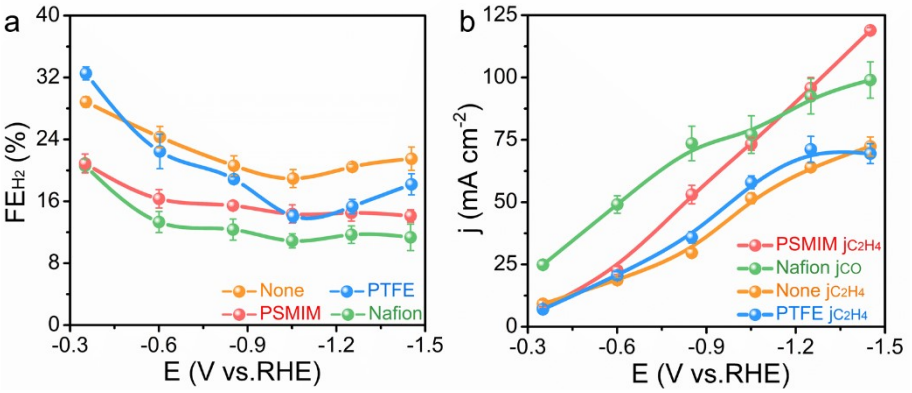

Figure S8 FEs of (a) H_2 on porous Cu NSs electrode modified with different types of organic polymer under applied potentials. (b) Partial current densities of main products on porous Cu NSs electrode modified with varying types of organic polymer.

In a membrane electrode assembly (MEA) with a working area of 2.25 cm^2 and a full cell voltage of -3.3 V, the stability of Nafion and PSMIM-modified porous Cu NSs electrodes for CO_2 electroreduction (ECO_2RR) was preliminarily tested using a 0.1 M $KHCO_3$ aqueous solution as the anodic electrolyte to evaluate their potential for practical applications. **Fig. S9a** shows the gas product distribution and current density vs. time trend for the Nafion-Cu NSs electrode during ECO_2RR. The main product of the Nafion-Cu NSs electrode is CO, with a Faraday efficiency (FE) of (46 ± 2)%, and it can stably operate for up to 20 hours at a current density of ~100 mA cm^{-2}. With the prolongation of reaction time, the FE of H_2 gradually increases while that of CO decreases. **Fig. S9b** shows the gas product distribution and current density vs. time trend for the PSMIM-Cu NSs electrode during ECO_2RR. The main product of the PSMIM-Cu NSs electrode is C_2H_4, with an FE of (45 ± 3)%, and it can stably operate for up to 70 hours at a current density of ~100 mA cm^{-2}. In the MEA system, the Nafion-Cu NSs electrode can operate stably for a much shorter time than the PSMIM-Cu NSs electrode, consistent with the results from a flow electrolysis cell. These experimental results further demonstrate that PSMIM-modified porous Cu NSs electrodes can efficiently and selectively catalyze CO_2 conversion to C_2H_4 with high stability. Therefore, the development of PSMIM-

modified porous Cu NSs electrodes has great potential to accelerate the practical application of porous Cu NSs electrodes for ECO_2RR to C_2H_4.

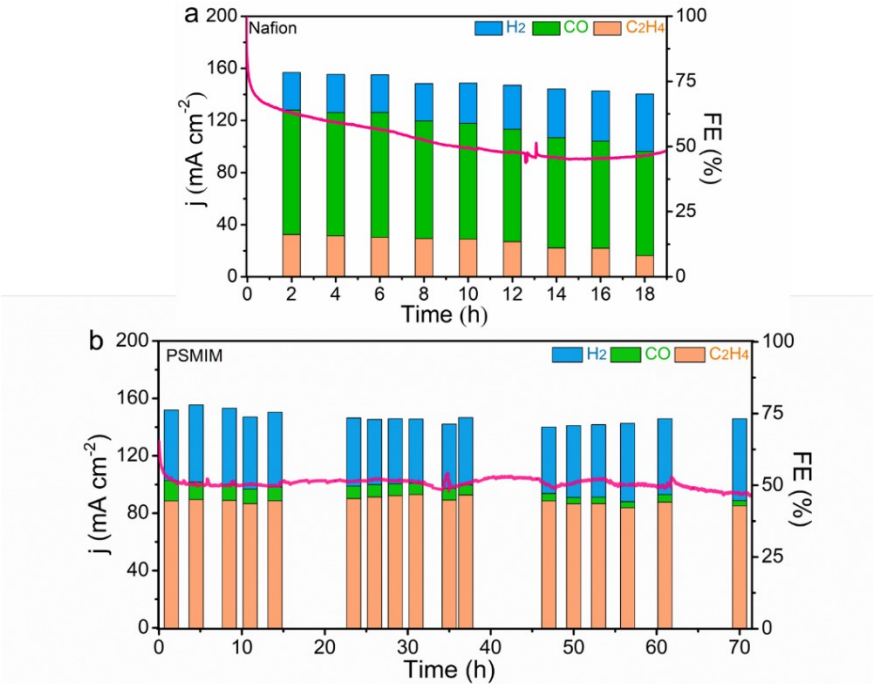

Figure S9 The ECO_2RR selectivity and stability of porous Cu NSs modified by (a) cationic organic polymer Nafion and (b) anionic organic polymer PSMIM.

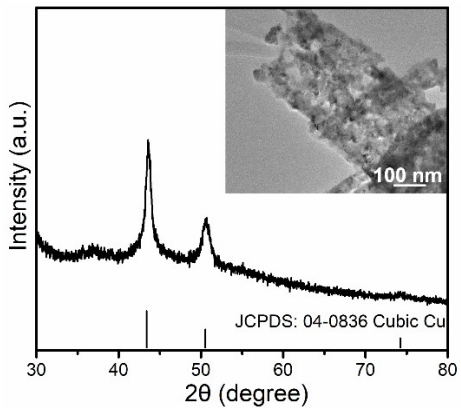

Figure S10 XRD pattern and TEM images of porous Cu NSs after ECO_2RR for 70 h in an MEA.

The structure and morphology of porous Cu NSs after ECO_2RR for 70 h are shown in **Figure S10**. The cubic Cu with porous nanosheet morphology is also detected after long-term durability, revealing the high structure stable property of porous Cu NSs during the ECO_2RR process.

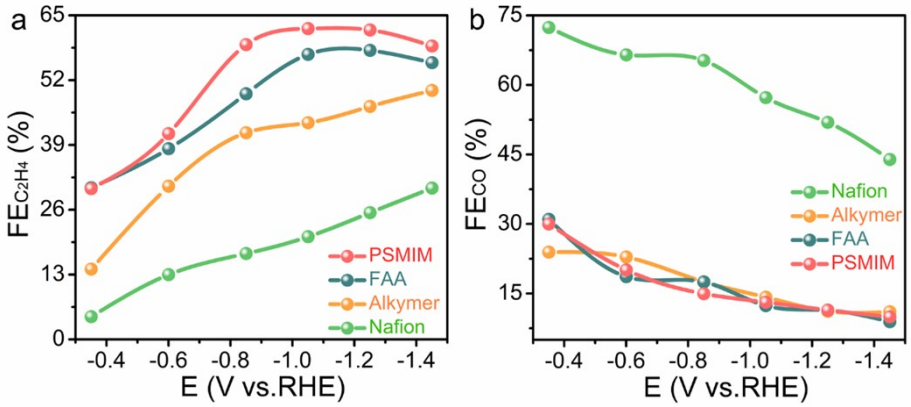

Figure S11 FEs for (a) C_2H_4 and (b) CO on porous Cu NSs modified with different types of organic polymer.

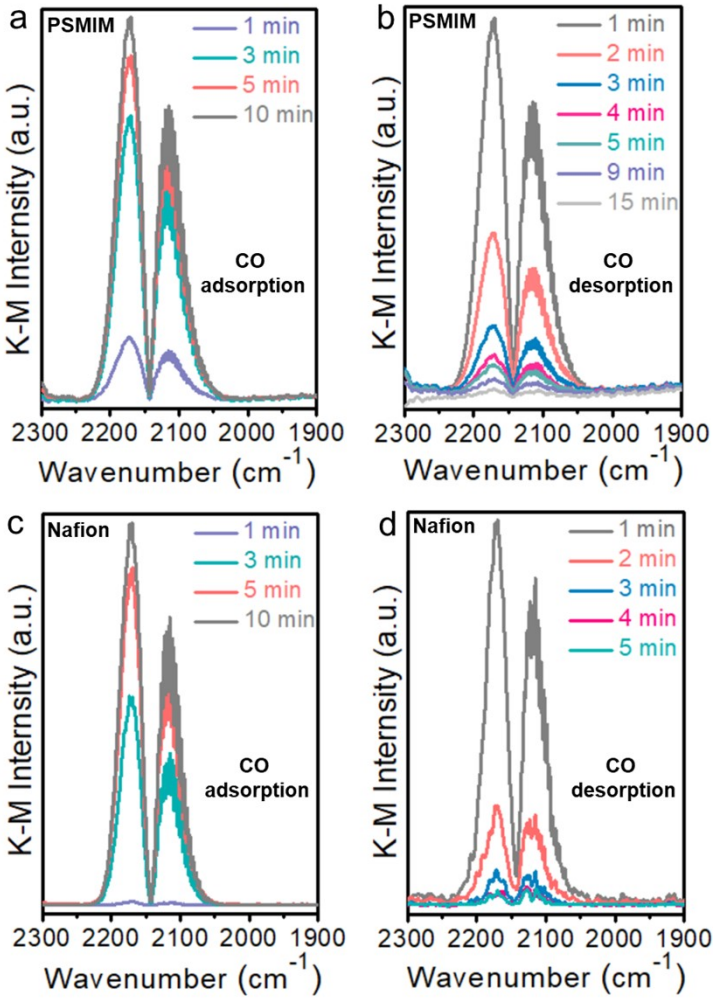

Figure S12 In-situ CO adsorption DRIFTS on (a) PSMIM-Cu NSs and (c) Nafion-Cu NSs. In-situ CO desorption DRIFTs on (b) PSMIM-Cu NSs and (d) Nafion-Cu NSs.

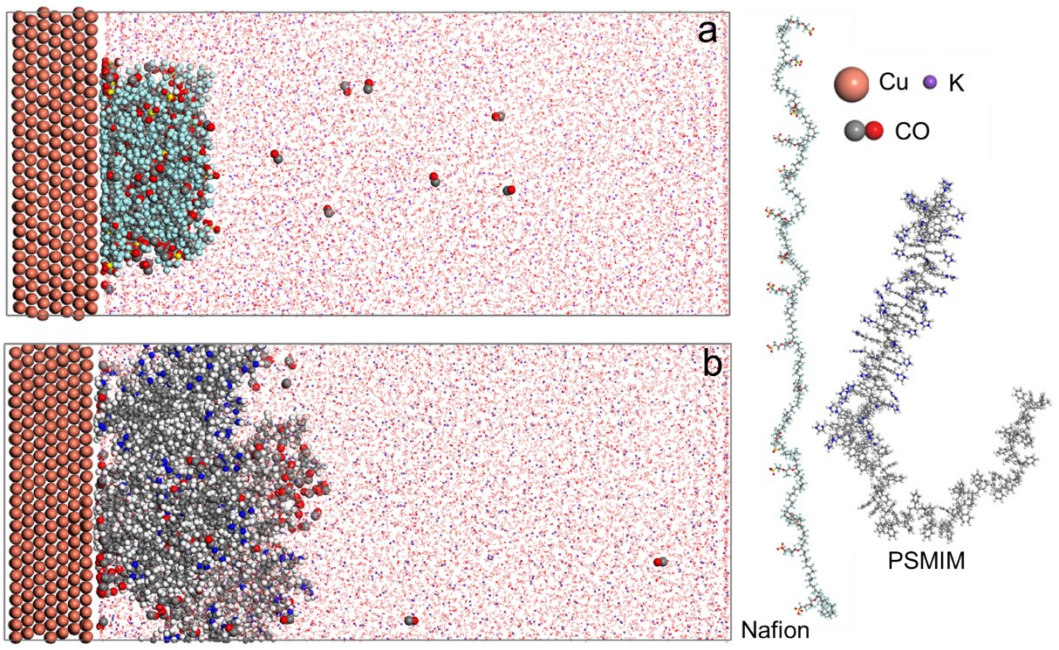

Figure S13 Molecular dynamics of the adsorption of CO on the Cu surface modified with (a) cationic organic polymer Nafion and (b) anionic organic polymer PSMIM.

Molecular dynamics simulations were used to explore the difference in the adsorption of CO, an intermediate in CO_2 electroreduction, on Cu surfaces modified by Nafion and PSMIM, and the results are shown in **Fig. S13**. The molecular dynamics simulation results showed that the adsorption energy of CO on the Nafion-modified Cu surface was -1453.58 kcal/mol, with an electrostatic interaction of −413.48 kcal/mol (**Fig. S13a**), while the adsorption energy of CO on the PSMIM-modified Cu surface was -1562.26 kcal/mol, with an electrostatic interaction of -757.58 kcal/mol (**Fig. S13b**). The above results indicate that CO is more easily adsorbed on the PSMIM-modified Cu surface. Combined with the molecular dynamics simulation results and the effect of Nafion and PSMIM on the selectivity of CO_2 electroreduction products on porous Cu NSs, it can be concluded that introducing functional additives in the catalytic layer is beneficial for regulating the local microenvironment, improving the adsorption ability of CO intermediates in ECO_2RR, and thus adjusting the selectivity of ECO_2RR products.

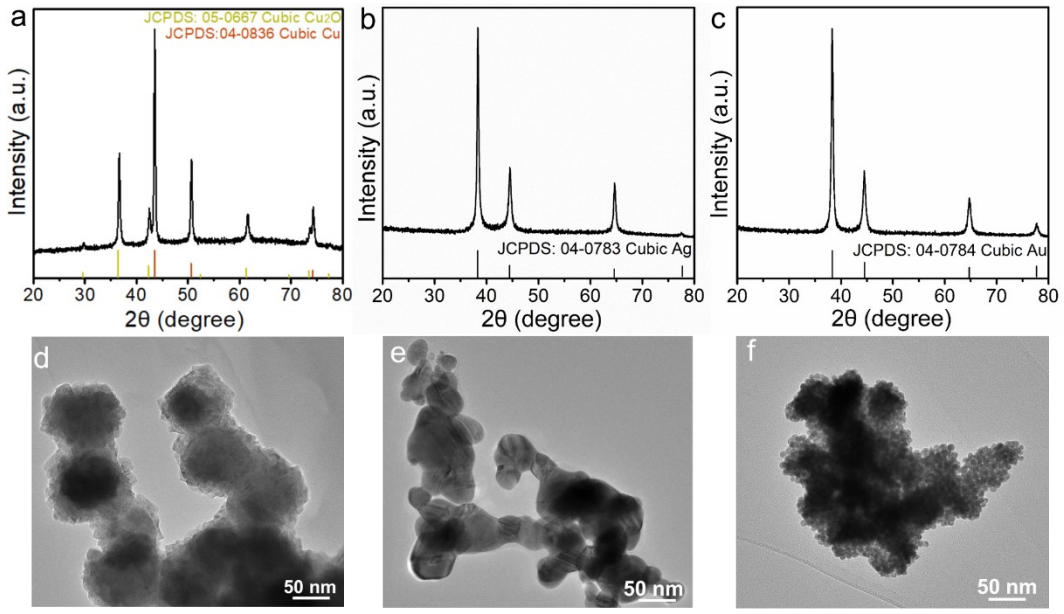

Figure S14 (a) XRD pattern, (d) TEM image of commercial Cu NPs. (b) XRD pattern, (e) TEM image of commercially available cubic-phase Ag NPs. (c) XRD pattern, (f) TEM image of Au NPs.

Fig. S14a shows the XRD pattern of commercial Cu NPs, from which it can be seen that the main phase is cubic Cu, and there is also a diffraction peak of cubic Cu_2O. The presence of the Cu_2O phase is due to the oxidation of the sample after long-term exposure to air. **Fig. S14d** shows the TEM photo of commercial Cu NPs, from which it can be seen that the size of commercial Cu NPs is about 100 nm, and small Cu NPs easily aggregate to form Cu nanospheres. **Figs. S14b** and **e** present the XRD pattern and TEM image, respectively, of commercially available cubic-phase Ag NPs, which exhibit irregular particle morphology in a bluish-gray color. **Fig. S14c** shows the XRD pattern of Au NPs, indicating that the prepared Au NPs are pure and well-crystallized cubic-phase Au. **Fig. S14f** shows the TEM image of the prepared Au NPs, revealing a size of approximately 5 nm, with small particles prone to aggregation due to their larger surface energy.

Reference

[1] W. Luc, J. Rosen, F. Jiao, Catal. Today, 2017, **288**, 79-84.